CrossMark

ORIGINAL PAPER

Influence of pH, Pb^{2+}, and temperature on the electrochemical dissolution of galena: environmental implications

Guoheng Jin[1,2] · Luying Wang[1,2] · Kai Zheng[1,2] · Heping Li[1] · Qingyou Liu[1]

Abstract We investigated the influence of pH, Pb^{2+}, and temperature on the electrochemical dissolution of galena. The experimental results showed the following: (1) Acidic or alkaline conditions stimulate galena electrochemical dissolution. The galena electrode corrosion current density (j_{corr}) increased from 0.072 to 0.143 µA·cm^{-2} as the pH decreased from 6.0 to 2.0 (promotion efficiency of 98.61 %) and from 0.066 to 0.132 µA·cm^{-2} as the pH increased from 8.0 to 12.0 (promotion efficiency of 100 %). (2) Pb(NO$_3$)$_2$ promotes galena electrochemical dissolution at low concentrations (<0.10 mol·L^{-1}) and inhibits it at high concentrations (>0.10 mol·L^{-1}) because Pb^{2+} has two different functions during galena electrochemical dissolution. (3) Higher temperatures are favorable for galena electrochemical dissolution. The galena j_{corr} increased from 0.143 to 0.226 µA·cm^{-2} as the temperature increased from 25 to 55 °C. These experimental results are of direct significance for the control of environmental pollution during galena weathering and mining activities.

Keywords Galena · pH · Temperature · Electrochemical · Environmental

✉ Qingyou Liu
liuqingyou@vip.gyig.ac.cn

1 Key Laboratory of High-Temperature and High-Pressure Study of the Earth's Interior, Institute of Geochemistry, Chinese Academy of Sciences, Guiyang 550002, China

2 University of Chinese Academy of Sciences, Beijing 100039, China

Introduction

The mineral galena (PbS) is an important sulfide lead mineral and is one of the most intensively studied sulfide minerals [1] because it is the main source of lead. Galena can be easily oxidized under human exploitation or in endemic geochemical processes, releasing Pb and other accompanying heavy metal ions (such as Zn, As, and Cd), resulting in heavy metal and acid drainage pollution. Due to the development of mining and metallurgical industries and due to increasing awareness of the requirement for environmental protection, environmental issues stemming from galena mining and processing activities are attracting increasing attention.

In nature, galena is primarily found in lead-zinc mines and coal. Lar et al. [2] found that in New Zurak, central Nigeria, the release of Pb and other potentially harmful elements (U, Cd, Se, Zn, and As) from galena mining activities has significantly contributed to the enrichment of these elements in the surrounding environment, including natural water bodies, allowing these elements to enter the human body through the food chain. During coal mining, processing, and utilization, Pb (which primarily associates with galena) is partially emitted into the atmosphere and partially partitioned into solid residues [3]. The accumulation of Pb in the human body can lead to a range of health problems and an increase in the risk of cancer [4]. More seriously, the various sources of pollution will remain for a very long time, even after all mining activities have ceased [5]. Luo et al. [6] used Pb isotopes to investigate the pollution of Pb in vegetable fields near a Pb-Zn mine that has been exploited for over 50 years without a tailing reservoir. The results showed that the vegetable fields were seriously polluted by As, Cd, and Pb. Specifically, Pb minerals were the major pollution sources, and aerosols were the main carrier of mining pollution. Some concentrations in the samples were above the regulatory levels and were not suitable for

agricultural areas. Many countries are suffering from environmental issues related to oxidized galena, and the main sources are abandoned sulfide mines or flotation tailings. In Tunisia, in the Jebel Hallouf-Sidi Bouaouane district, more than 500 million tons of galena (and associated sphalerite, pyrite, and marcasite) flotation tailings have been eroded by wind and running waters, leading to high mobilities of heavy metals (Pb, Zn, and Cd) to flood areas, exceeding environmental norms, especially in the case of soils on the eastern side of Jebel Hallouf Mountain [7]. In France, the Deule River fluvial environment has experienced severe degradation over the past several years. Boughriet et al. [8] revealed that a former smelting plant (Metaleurop) was responsible for the Deule River's environmental issue. Because Metaleurop smelter yielded lots of sulfide/organic fraction to the Deule River, the resulting Deule River sediment primarily consists of galena (PbS), wurtzite (ZnS), and pyrite (FeS$_2$). In Broken Hill, Australia, Kristensen et al. [9] investigated an unusual source of environmental lead contamination, finding the emission and deposition of lead and zinc concentrates along train lines into and out of Australia's oldest silver-lead-zinc mine. They found that a significant amount of ore was lost to the adjoining environment, resulting in elevated concentrations of lead (695 mg·kg^{-1}) and zinc (2230 mg·kg^{-1}) in the soil immediately adjacent to the train lines. In fact, the reason for this issue is that the lead-zinc ore particles from uncovered wagons during the local mining operations contaminated hundreds of kilometers of the train lines.

As shown in the above examples, the reason for the environmental issues coming from galena is galena weathering. Lara et al. [10] studied the weathering mechanisms of galena in simulated calcareous soil and its environmental implications. They found that galena weathering leads to the formation of lead phases (e.g., PbSO$_4$, PbCO$_3$) with a higher bioaccessibility than galena, which increases the lead mobility and change its specific chemical hazard. At the initial oxidation stage, an anglesite-like phase formed, leading to the partial mineral passivation. However, the anglesite-like phase was unstable and then transformed into a cerussite-like phase. It is undeniable that the weathering process of galena in nature is an electrochemical process [11]. Mikhlin et al. [12] studied the electrochemical dissolution of galena and proposed that the predominant donor-like defects in the disordered reaction layers inhibit PbS oxidation and promote metallic lead deposition in the course of potential cycling. Fornasiero et al. [13] studied the oxidation of galena and proposed that the zeta potential changes occurring during the surface oxidation may be due to the colloidal particles that formed by the readsorption of Pb^{2+}. Galena weathering is often seen in acidic conditions in nature; hence, many studies of galena electrochemical dissolution are conducted in acidic conditions. The anodic dissolution process in an acid system is typically expressed as follows [14]: PbS→Pb^{2+}+S^0+2e$^-$, and O$_2$ was

reduction on the cathode reaction: O$_2$+4H$^+$+4e$^-$=2H$_2$O. Paul et al. [15] and Nicol et al. [16] conducted detailed studies of the anodic electrochemical dissolution and cathodic reduction of galena. They proposed a mechanism involving a sulfur intermediate (represented as S$^-$) for the above-proposed anodic dissolution and noted that the morphology of the anodically produced sulfur affects the active-passive behavior of galena. The rate of the cathodic reduction is strongly dependent on the amount of sulfur present and its history. To date, many reports have identified intermediate sulfur species, their surface characteristics, and their semiconducting properties at different positive potentials using chronoamperometry [17], cyclic voltammetry [18–20], and electrochemical impedance spectroscopy (EIS) [21]. Various surface techniques have also been used, such as Raman spectroscopy [22], scanning tunneling microscopy (STM) [23], X-ray photoelectron spectroscopy (XPS) [24], in situ Fourier transform infrared (FTIR) spectroscopy [25], and synchrotron radiation excited photoelectron spectroscopy (SR-XPS) [26].

Temperature, pH, and Pb^{2+} (an important source of accumulated Pb^{2+} from galena weathering) are the primary factors affecting the weathering process of galena. To our knowledge, no quantitative data have been reported on the influence of pH, temperature, and Pb^{2+} on the weathering process of galena (electrochemical dissolution). Therefore, the goal of this study is to examine the electrochemical response of a large sample of galena under different pH values, temperatures, and Pb^{2+} concentrations and to obtain quantitative electrochemical dissolution parameters to understand the extent to which the above factors influence the galena weathering process. These experimental results are of direct significance for the control of environmental pollution during galena weathering and mining activities.

Experimental

Electrode preparation

High-quality natural galena was obtained from the Huize Pb-Zn deposit of Yunnan Province, China. X-ray powder diffraction analysis confirmed that the ore sample was composed of PbS and ZnS, and electron microprobe analysis confirmed that the Pb, S, and Zn contents (wt.%) were 86.53, 13.39, and 0.0064 %, respectively. The galena electrode was prepared by cutting the galena sample into approximately cubic pieces with working areas of 0.25 cm^2, avoiding visible imperfections as much as possible. After cleaning the pieces in detergent, ethanol, and ultrapure water, the specimens were placed on an epoxy resin, and each was connected to a copper wire using silver paint on its back face, exposing only one face of the electrode to the solution. Prior to each test, the mineral electrode was polished with 1200$^{\#}$ carbide paper to obtain a

fresh surface, degreased using alcohol, rinsed with deionized water, and dried in a stream of air.

Electrochemical measurements

Electrochemical measurements were performed using a computer-controlled electrochemical measurement system on a conventional three-electrode electrolytic cell with platinum as an auxiliary electrode and the galena electrode as the working electrode (WE). A saturated calomel electrode (SCE) was used as a reference electrode for all of the electrochemical tests. All potentials quoted in this study are relative to the SCE (242 mV vs. standard hydrogen electrode) unless otherwise noted. The reference electrode was connected to a Luggin capillary to minimize the IR drop. The electrolytes were prepared from deionized water by adding different quantities of $Pb(NO_3)_2$ and H^+ (adjusted with HNO_3 and NaOH). The working, auxiliary and reference electrodes were placed in the same location to ensure a uniform spatial relationship.

Polarization curves were obtained by scanning the electrode potential from −250 to +250 mV (vs. open current potential, OCP) at a scan rate of 10 mV·s^{-1}. EIS tests were performed at OCP and in the frequency range of 0.001~10,000 Hz with a peak-to-peak amplitude of 10 mV, and then, ZSimpWin 3.20 (2004) software was used to fit the impedance data. To ensure reproducibility, at least three identical experiments were conducted to ensure that the reported results were reproducible (i.e., the random errors of all three identical experimental results were within tolerance), and the results reported in this study are the averages of these repetitions.

Prior to obtaining the polarization curves and conducting EIS, OCP tests were performed. During the OCP tests, the electrode potential increased for 5 min and then reached a quasi-steady state, defined here as a change of less than 2 mV per 300 s. The electrode was then stabilized for 400 s, and this potential was recorded as the OC potential. During the second and third replicates, if the potential was not within ±5 mV of the value from the first test at the quasi-steady state, then the OCP test was terminated, and a new test was performed until the OC potential from the first test was obtained when stabilized for 400 s.

Results and discussion

Influence of pH

As is well known, the long-term weathering of galena results in acid mine drainage; thus, galena weathering typically occurs under acidic conditions. In some instances, galena can also occur under neutral to slightly alkaline conditions [27] and even under fully alkaline conditions, for example, in some landfill leachate [28] or ash-covered tailings [29]. Thus, in this study, pH values from 2.0 to 12.0 were selected to study the influence of pH on galena electrochemical dissolution.

Figure 1a shows the polarization curves for the galena electrode in nitric acid (pH 2.0, 4.0, and 6.0) or sodium hydroxide (pH 8.0, 10.0, and 12.0) solutions at a scan rate of 10 mV·s^{-1}. It is clear that with increasing pH, the polarization curves for the corrosion potential shift to the negative direction.

The corrosion potential (E_{corr}), corrosion current density (j_{corr}), and Tafel slopes of the anode (b_a) and cathode (b_c) were derived from the polarization curves based on the extrapolation methods outlined in the literature [30]. Furthermore, the polarization resistance values, R_p, were calculated from the Stern-Geary equation: $R_p = b_a b_c/[2.3 j_{corr}(b_a + b_c)]$ [31]. The calculated polarization values are listed in Table 1.

When the electrolyte contained acid, the j_{corr} of the pyrite electrode increased from 0.072 to 0.143 μA·cm^{-2} as the pH decreased from 6.0 to 2.0, indicating that higher acidity accelerates galena corrosion, and the promotion efficiency (η) was 98.61 %. In this study, η is defined as $\eta = (j_{corr} - j_{corr}^0)/j_{corr}^0$, which is used as the inhibition efficiency in materials science [32, 33]. Here, j_{corr}^0 and j_{corr} are the corrosion current density before and after the pH change, respectively. This study suggests that the drive power comes from the galena electrode polarization resistance reduction, which decreased from 750.8 to 268.7 Ω·cm^2. This phenomenon is explained as follows. When the electrolyte contained acid, galena acted as the anode and was oxidized (reaction (1)). S^0 is produced and can be absorbed on the galena electrode surface, and S^0 dissolution is favored by stronger acidity. At the cathode, O_2 was reduced as reaction (2); higher acidity is clearly beneficial for this reaction as well. Thus, the anodic and cathodic Tafel slopes decrease.

When the electrolyte contained alkali, as in the case of acid, the galena electrode j_{corr} increased from 0.066 to 0.132 μA·cm^{-2} as the alkalinity increased from pH 8 to 12. In this case, the promotion efficiency (η) was 100 %. In contrast to the case of increasing acidity, the decrease in the galena polarization resistance with increasing alkalinity was due to the decrease in the galena anodic Tafel slope, despite the concurrent increase in the cathodic Tafel slope. This galena electrode behavior is explained as follows. When the electrolyte contained alkali, O_2 was reduced via reaction (3) on the cathode. The presence of more OH^- ions is unfavorable for reaction (3), increasing the cathodic Tafel slope. However, the presence of more OH^- ions is favorable
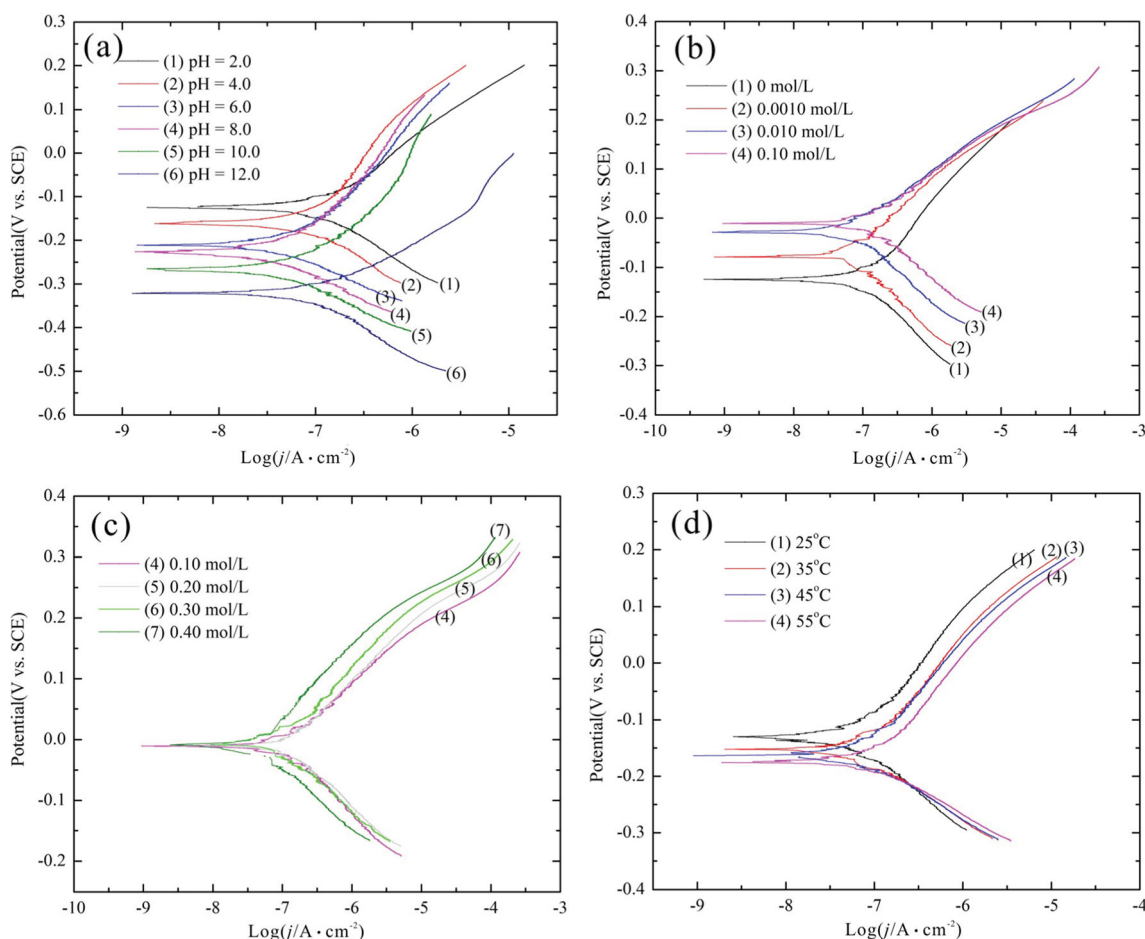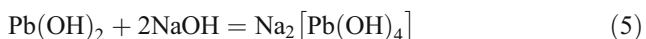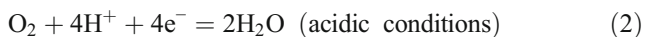
Fig. 1 Potentiodynamic curves of the galena electrode under different pH values (**a**); concentrations of Pb(NO₃)₂ (**b, c**); and temperatures (**d**)

for galena anodic oxidation, according to reactions (4) and (5), decreasing the anodic Tafel slope.

Anode:

$$PbS \rightarrow Pb^{2+} + S^0 + 2e^- \qquad (1)$$

Cathode:

$$O_2 + 4H^+ + 4e^- = 2H_2O \quad (\text{acidic conditions}) \qquad (2)$$

$$O_2 + H_2O + 2e^- = HO_2^- + OH^- (\text{alkaline conditions}) \qquad (3)$$

$$Pb^{2+} + 2OH^- = Pb(OH)_2 \qquad (4)$$

$$Pb(OH)_2 + 2NaOH = Na_2[Pb(OH)_4] \qquad (5)$$

EIS has been widely applied to the study of the characteristics of electrodes and electrochemical reactions [34]. In this section, EIS studies were used to confirm the above-obtained polarization curves and to clarify the mechanism of the electrochemical oxidation of galena.

Figure 2b, c presents the Nyquist plots for galena under nitric acid (pH 2.0, 4.0, and 6.0) and sodium hydroxide (pH 8.0, 10.0, and 12.0) solutions. The Nyquist plots are composed of two capacitive loops. The loop at high frequencies is attributed to the charge transfer resistance R_t, which may correspond to the resistance between the galena and the outer Helmholtz plane. The lower-frequency capacitive loop, which is slightly distorted, is related to the combination of a pseudo-capacitance impedance (due to the passive layer) and a resistance R_f. The deviation from an ideal semicircle is attributed to the frequency dispersion and the inhomogeneities of the passive layer surface. The related electrochemical

Table 1 Electrochemical parameters of PbS under different pH values

pH	E_{corr} (mV)	j_{corr} (µA·cm⁻²)	b_c (mV)	b_a (mV)	R_p (Ω·cm²)
2.0	−143.60	0.143	144.71	228.14	268.7
4.0	−169.14	0.112	170.56	297.67	422.8
6.0	−210.82	0.072	193.67	347.32	750.8
8.0	−227.87	0.066	160.05	260.37	654.5
10.0	−258.32	0.088	166.83	205.42	454.9
12.0	−321.53	0.132	181.11	125.74	243.5

E_{corr} corrosion potential, j_{corr} corrosion current density, b_a Tafel slopes of the anode, b_c Tafel slopes of the cathode, R_p polarization resistance values
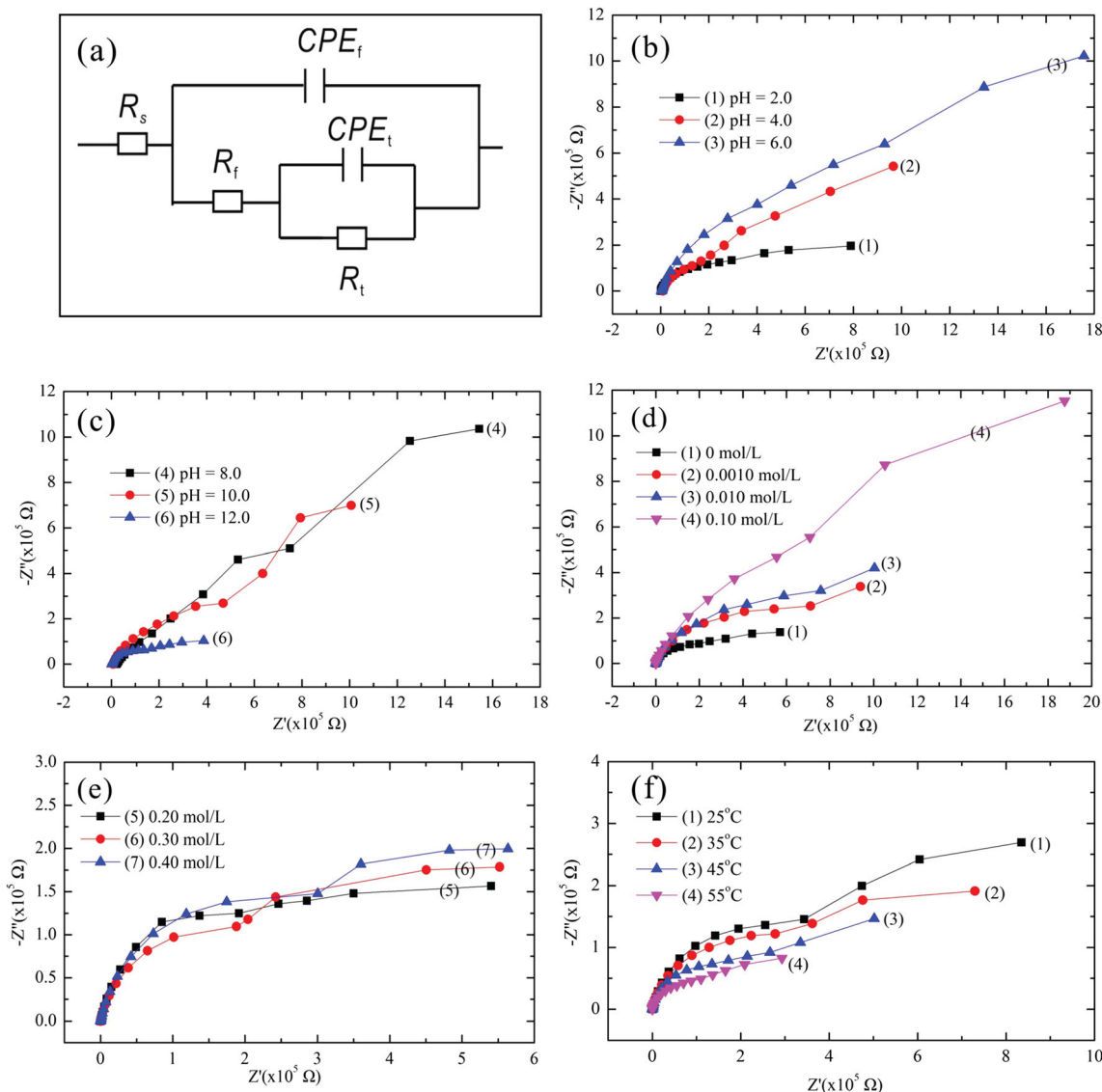
Fig. 2 Equivalent circuit for the galena electrode/electrolyte at OCP (**a**). Nyquist plots of the galena electrode under different pH values (**b**, **c**). Concentrations of Pb(NO$_3$)$_2$ (**d**, **e**). Temperatures at OCP (**f**)

equivalent circuit (EEC) used to model the galena/electrolyte interface is shown in Fig. 2a in which R_s is the ohmic resistance of solution, R_t is the charge transfer resistance, R_f is the passive film resistance, and CPE$_t$ and CPE$_f$ represent the constant phase element used to replace the charge transfer capacitance at the double layer (C_t) and the passive film capacitance (C_f), respectively. Constantin and Chirita [35], as well as Ouyang et al. [36], used this model to explain the oxidative dissolution of pyrite in acidic media, and Pang et al. [37] provided a detailed theoretical explanation of this EEC model. Because the equivalent circuits provide a means of describing the electrochemical processes that occur at the electrode/electrolyte interface, any models derived from these circuits are only tentative [38]. Therefore, different EECs were used to fit the EIS data, and the results are shown in Tables 2, 6, and 6.

These tables show that the proposed model in Fig. 2a provided the best fit among the EECs considered.

The impedance parameters obtained by fitting the EIS data to the equivalent circuit are listed in Table 2. For the galena double layer in acidic (alkaline) electrolyte, increasing the acidity (alkalinity) led to a decrease in all the R_t values and an increasing trend for the double-layer capacitance CPE$_t$, Y_0. The decrease in the R_t values indicates that ions can be easily transported through the double-charge layer, and the increase in CPE$_t$, Y_0 can be attributed to the increase in the local dielectric constant of the electrical double layer. The high capacitance and low resistance of the double layer indicate that increasing the acidity or alkalinity enhances galena electrochemical oxidation, as reflected in the polarization curve results, namely, higher acidity/alkalinity accelerates galena

Table 2 Model parameters for different pH values for the equivalent circuit shown in Fig. 2a

pH	CPE_t, Y_0 ($S \cdot cm^{-2} \cdot s^{-n}$)	n	R_t ($\Omega \cdot cm^2$)	CPE_f, Y_0 ($S \cdot cm^{-2} \cdot s^{-n}$)	n	R_f ($\Omega \cdot cm^2$)
2.0	4.276×10^{-5}	0.8085	7.182×10^4	4.354×10^{-4}	0.9622	1.103×10^5
4.0	3.782×10^{-5}	0.8019	7.326×10^4	2.001×10^{-4}	0.8772	2.661×10^5
6.0	2.757×10^{-5}	0.8029	2.344×10^5	1.102×10^{-4}	0.8403	5.782×10^5
8.0	3.736×10^{-5}	0.7918	2.219×10^5	2.007×10^{-4}	1	2.953×10^5
10.0	3.854×10^{-5}	0.7779	1.266×10^5	3.620×10^{-4}	0.7775	4.129×10^5
12.0	5.319×10^{-5}	0.7897	8.027×10^4	8.239×10^{-4}	0.9491	6.295×10^4

CPE_t, Y_0 constant phase element used to replace the charge transfer capacitance at double-layer capacitance, CPE_f constant phase element used to replace the charge transfer capacitance at passive film capacitance, n dimensionless number, R_t the charge transfer resistance, R_f passive film resistance

electrochemical corrosion. For the galena passive film, when the electrolyte was acidic, increasing the acidity decreased R_f and increased CPE_f, Y_0. The high capacitance and low resistance of the films on the specimens indicate the relatively low robustness of the passive film. Meanwhile, when the electrolyte was alkaline, increasing the alkalinity increased CPE_f, Y_0, but R_f followed a different trend, initially increasing and then decreasing. This difference in behavior is a result of the poorly soluble $Pb(OH)_2$ changing into soluble $Na_2[Pb(OH)_4]$ at higher alkalinity. In this study, this transition occurred as the pH increased from 10.0 to 12.0. All of these results are in good agreement with the polarization results.

Influence of Pb^{2+}

An electrochemical interaction is an oxidation-reduction reaction; thus, the characteristics of the electrolyte ions have an important influence on the electrochemical dissolution. In general, oxidizing ions (such as Fe^{3+}) in an electrolyte prompt electrochemical interactions. Pb^{2+} ions also act as oxidizing ions. Most ions of this type present in nature come from galena oxidation and constitute one of the polluting ions in mine areas. According to Eqs. (1) and (4), Pb^{2+} is both an oxidizing ion and one of the product ions. Thus, it should have distinctive effects on galena electrochemical dissolution. Therefore, in this study, different concentrations of Pb^{2+} were selected to investigate its influence on galena electrochemical dissolution.

Figure 1b, c presents the polarization curves for the galena electrode under different $Pb(NO_3)_2$ concentrations at a scan rate of 10 mV·s^{-1}. The galena polarization parameters found by extrapolation are shown in Table 3.

When $Pb(NO_3)_2$ was present in the range of 0 to 0.10 mol·L^{-1}, the galena electrode j_{corr} increased with the $Pb(NO_3)_2$ concentration. When the electrolyte contained a very small amount of $Pb(NO_3)_2$ (0.0010 mol·L^{-1}), j_{corr} increased from 0.143 to 0.182 μA·cm^{-2}, with a promotion efficiency (η) of 27.27 %. This value continued to increase, reaching 0.324 μA·cm^{-2} for a $Pb(NO_3)_2$ concentration of 0.10 mol·L^{-1}, at which point the promotion efficiency (η) was 126.57 %. This occurs

because the galena polarization resistance decreases at higher concentrations of $Pb(NO_3)_2$; specifically, R_f decreased from 268.7 to 127.3 $\Omega \cdot cm^2$ for these concentrations. At the anode, galena was oxidized according to reaction (1), and Pb^{2+} was released. The released Pb^{2+} (including that from the added $Pb(NO_3)_2$) is further reduced to Pb (reaction (6)). It is important to note that Pb^{2+} ions have two functions: facilitating Pb^{2+} reduction (reaction (6)) and inhibiting galena oxidation (reaction (1)). Considering these two functions together, as the concentration of Pb^{2+} ions increased from 0 mol·L^{-1} to a relatively low value, the reduction of Pb^{2+} was dominant. Thus, higher concentrations of Pb^{2+} are favorable for the reduction of Pb^{2+}, therefore, encouraging the anodic oxidization of galena. This oxidization corresponds to a decrease in the galena anodic Tafel slope. At the cathode, the dissolution of O_2 was suppressed, according to reaction (2), and Pb^{2+} is also reduced according to reaction (6) when the electrolyte contains $Pb(NO_3)_2$. It is worth noting that the O_2 reduction is dominant when the concentration of $Pb(NO_3)_2$ is very low (in this study, $0 \sim 0.10$ mol·L^{-1}). Furthermore, the amount of available oxygen in solution will decrease as the amount of added $Pb(NO_3)_2$ increases. Regarding this oxygen solubility phenomenon, Moslemi et al. [39] reported that the presence of chloride and sulfate ions causes a reduction in the amount of available oxygen in solution, and Geng and Duan [40] provided a detailed theoretical explanation and mathematical derivation of this phenomenon. Oxygen is a strong oxidant and hence a decrease in the amount of chloride and sulfate ions present would inhibit the oxygen reduction, leading to an increase in the galena cathodic Tafel slope:

$$Pb^{2+} + 2e^- \rightarrow Pb \quad E = -0.1262 \text{ V} \tag{6}$$
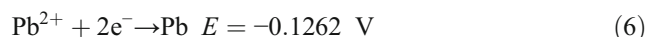
As the data in Table 3 show, when the electrolyte $Pb(NO_3)_2$ is present in concentrations above 0.10 mol·L^{-1}, the galena polarization resistance increases from 127.3 to 391.8 $\Omega \cdot cm^2$ with the increase in electrolyte concentration of $Pb(NO_3)_2$ from 0.10 to 0.40 mol·L^{-1}. A lower polarization resistance led to a higher corrosion current density, and the corresponding values were 0.324 and 0.059 μA·cm^{-2}, respectively. The above results reveal that higher concentrations of $Pb(NO_3)_2$

Table 3 Electrochemical parameters of PbS under different concentrations of Pb(NO$_3$)$_2$

Concentration (mol·L^{-1})	E_{corr} (mV)	j_{corr} (µA·cm^{-2})	b_c (mV)	b_a (mV)	R_p (Ω·cm^2)
0	−143.60	0.143	144.71	228.14	268.7
0.001	−58.43	0.182	170.30	187.34	213.1
0.010	−16.32	0.225	224.55	158.56	179.6
0.100	3.03	0.324	320.01	134.78	127.3
0.200	1.89	0.086	107.80	109.40	274.7
0.300	−3.18	0.082	102.03	112.34	283.5
0.400	−7.12	0.059	98.47	115.54	391.8

E_{corr} corrosion potential, j_{corr} corrosion current density, b_a Tafel slopes of the anode, b_c Tafel slopes of the cathode, R_p polarization resistance values

inhibit galena electrochemical dissolution, and the inhibition efficiency (η) was 58.74 % when Pb(NO$_3$)$_2$ increased from 0 to 0.40 mol·L^{-1}.

This behavior can be explained as follows. The reduction of Pb^{2+} ions to Pb will dominate because of their high concentration at the cathode, decreasing the cathode Tafel slope. However, the high concentration of Pb^{2+} ions also dramatically inhibits anodic oxidation.

To better understand the mechanism of galena electrochemical dissolution under different Pb^{2+} concentrations, EIS experiments were conducted. Figure 2d, e presents the Nyquist plots for galena under different concentrations of Pb(NO$_3$)$_2$. All the Nyquist plots are composed of two capacitive loops: one corresponding to the resistance between the galena and the outer Helmholtz plane and one related to the combination of a pseudo-capacitance impedance (due to the passive layer). The EEC shown in Fig. 2a was used to model the galena/electrolyte interface, and the physical significance of the different model elements was clarified in "Influence of pH" section. The impedance parameters obtained by fitting the EIS data to the equivalent circuit are listed in Table 6.

When the Pb(NO$_3$)$_2$ concentration is in the range of 0 to 0.10 mol·L^{-1}, for the galena double layer, increasing the concentration of Pb(NO$_3$)$_2$ decreased the galena R_t values and increased the double-layer capacitance CPE$_t$, Y_0 values. The

high capacitance and low resistance of the double layer indicate that increasing the Pb(NO$_3$)$_2$ concentration prompted galena electrochemical oxidation, which is in agreement with the polarization curve results. For the galena passive film, increasing Pb(NO$_3$)$_2$ increases R_f and decreases CPE$_f$, Y_0. The low capacitance and high resistance of the films on the specimens indicate the relative robustness of the passive film, confirming more S^0 film rose.

When Pb(NO$_3$)$_2$ is present in the electrolyte at levels above 0.10 mol·L^{-1}, increasing Pb(NO$_3$)$_2$ decreases R_t. It appears that increasing Pb(NO$_3$)$_2$ is favorable for galena electrochemical dissolution. However, it should be mentioned that CPE$_t$, Y_0 exhibited a different trend in which it decreased as Pb(NO$_3$)$_2$ increased. A decrease in the R_t and CPE$_t$, Y_0 values would indicate that the transfer charges had a lower transfer resistance at the double layer, but the real transfer charges did not increase with increasing Pb(NO$_3$)$_2$. This behavior results from the thicker passive film present on the galena surface, which is apparent from increase in the R_f values as Pb(NO$_3$)$_2$ increased over this concentration range.

Influence of environmental temperature

During the galena formation and deposition processes that occur in nature, the geological conditions often have different

Table 4 Model parameters for different concentrations of Pb(NO$_3$)$_2$ for the equivalent circuit shown in Fig. 2a

Concentration (mol·L^{-1})	CPE$_t$, Y_0 (S·cm^{-2}·s^{-n})	n	R_t (Ω·cm^2)	CPE$_f$, Y_0 (S·cm^{-2}·s^{-n})	n	R_f (Ω·cm^2)
0	4.276×10^{-5}	0.7969	7.182×10^4	4.345×10^{-4}	0.9622	1.103×10^5
0.001	7.103×10^{-5}	0.8211	6.842×10^4	4.023×10^{-4}	1	1.720×10^5
0.010	1.160×10^{-4}	0.8196	3.024×10^4	3.760×10^{-5}	1	2.010×10^5
0.100	1.302×10^{-4}	0.8342	7.183×10^3	3.242×10^{-5}	1	2.342×10^5
0.200	1.016×10^{-4}	0.8298	4.546×10^3	4.542×10^{-5}	1	2.380×10^5
0.300	7.230×10^{-5}	0.8082	4.457×10^3	6.104×10^{-5}	0.7854	2.697×10^5
0.400	6.695×10^{-5}	0.8260	3.820×10^3	7.869×10^{-5}	0.7748	2.842×10^5

CPE$_t$, Y_0 constant phase element used to replace the charge transfer capacitance at double-layer capacitance, CPE$_f$ constant phase element used to replace the charge transfer capacitance at passive film capacitance, n dimensionless number, R_t the charge transfer resistance, R_f passive film resistance

Table 5 Electrochemical parameters of PbS under different temperatures

Temperature (°C)	E_{corr} (mV)	j_{corr} ($\mu A \cdot cm^{-2}$)	b_c (mV)	b_a (mV)	R_p ($\Omega \cdot cm^2$)
25	−143.60	0.143	144.71	228.14	268.7
35	−147.23	0.170	129.42	207.27	203.3
45	−149.72	0.210	113.42	201.97	150.4
55	−166.26	0.226	96.55	208.47	127.1

E_{corr} corrosion potential, j_{corr} corrosion current density, b_a Tafel slopes of the anode, b_c Tafel slopes of the cathode, R_p polarization resistance values

temperatures. Temperature can affect the thermodynamics and kinetics of an interaction and is undoubtedly an important electrochemical factor. Considering typical geological environments, four different temperatures, 25, 35, 45, and 55 °C, were selected to investigate the influence of temperature on galena electrochemical dissolution.

Figure 1d shows the polarization curves for the galena electrode under different temperatures at a scan rate of 10 mV·s^{-1}. The galena polarization parameters found by extrapolation are shown in Table 5. Table 5 shows that the polarization resistance decreased from 268.7 to 127.1 $\Omega \cdot cm^2$ as the temperature increased from 25 to 55 °C. Specifically, the lower polarization resistance intensified the galena electrochemical corrosion and resulted in an increase in corrosion current density from 0.143 to 0.226 $\mu A \cdot cm^{-2}$. The promotion efficiency (η) was 58.04 %. Chirita et al. [41] reported a similar finding, namely, that higher temperature accelerates electrochemical dissolution, while investigating pyrite electrochemical oxidization at different temperatures. This behavior is explained by the fact that increasing temperature causes a conversion of internal energy into electrochemical energy, decreasing all the anodic and cathodic polarization resistances. This explanation is consistent with the anodic and cathodic Tafel slope results.

EIS experiments were conducted to study the effect of temperature on galena electrochemical behavior, and the Nyquist plots for galena at different temperatures are shown in Fig. 2f. The same EEC shown in Fig. 2a was used to model the galena/electrolyte interface, and the impedance parameters obtained by fitting the EIS data to the equivalent circuit are listed in

Table 6. The results show that the double-layer charge transfer resistance decreased and the capacitance increased as the temperature increased, suggesting that charge transfer was facilitated at the double layer. For the galena passive film, increasing the temperature led to a smaller R_f value and a larger CPE_f, Y_0 value. The larger capacitance and smaller resistance of the films on the specimens indicate the relative weakness of the passive film, which was confirmed by the reduced development of S^0 film. All of these results agree with the polarization curve results.

Implications for environmental pollution and treatment at mines

(1) In nature, galena is often surrounded by acidic conditions and is occasionally surrounded by alkaline conditions during long-term weathering. The above experimental results indicate that when galena is exposed to acidic or alkaline conditions, its electrochemical corrosion will be stimulated, which will result in more severe environmental problems. Therefore, it is critical for mine area environmental treatment to occur before the mine drainage reaches areas that are acidic or alkaline, especially before acid mine drainage (AMD) (pH<2.0) formation.

(2) Pb^{2+} ions are often observed in galena mine area fluids, and their presence is unfavorable for galena mine area environmental remediation because even a very small amount of Pb^{2+} (0.0010 mol·L^{-1}) will strongly stimulate galena electrochemical dissolution. However, when the

Table 6 Model parameters for different temperatures for the equivalent circuit shown in Fig. 2a

Temperature (°C)	CPE_t, Y_0 ($S \cdot cm^{-2} \cdot s^{-n}$)	n	R_t ($\Omega \cdot cm^2$)	CPE_f, Y_0 ($S \cdot cm^{-2} \cdot s^{-n}$)	n	R_f ($\Omega \cdot cm^2$)
25	4.276×10^{-5}	0.8085	7.182×10^4	4.354×10^{-4}	0.9622	1.103×10^5
35	5.771×10^{-5}	0.8013	7.035×10^4	5.554×10^{-4}	0.9464	6.259×10^4
45	6.347×10^{-5}	0.8009	2.186×10^4	5.988×10^{-4}	0.6597	3.302×10^4
55	6.644×10^{-5}	0.7955	3.689×10^3	7.288×10^{-4}	0.5236	1.077×10^4

CPE_t, Y_0 constant phase element used to replace the charge transfer capacitance at double-layer capacitance, CPE_f constant phase element used to replace the charge transfer capacitance at passive film capacitance, n dimensionless number, R_t the charge transfer resistance, R_f passive film resistance

Pb^{2+} concentration reaches a relatively large value (in this study, near 0.10 mol·L^{-1}), galena corrosion will be inhibited, which suggests that the Pb^{2+} ion accumulation rate will be slow.

(3) Temperature is an important factor affecting galena electrochemical dissolution, serving to accelerate it. In different galena mine areas, temperature differences occur due to differences in regions and seasons. This may cause differences in the observed pollution levels.

These findings provide information and a scientific basis, as well as new paths, for controlling pollution in mining areas caused by galena.

Conclusions

Based on the established electrochemical parameters of galena, the following conclusions could be derived:

(1) Higher acidities or alkalinities stimulate galena electrochemical dissolution. Specifically, galena electrode j_{corr} increased from 0.072 to 0.143 µA·cm^{-2} when the pH decreased from 6 to 2, at a promotion efficiency of 98.61 %, and from 0.066 µA·cm^{-2} to 0.132 µA·cm^{-2} when the pH increased from 8 to 12, at a promotion efficiency of 100 %. These phenomena result from the presence of a large quantity of H^+ or OH^- acting to decrease the charge transfer resistance in the double layer and decreasing the passive resistance at the electrode surface, although the interaction mechanism was different in the cathode.

(2) $Pb(NO_3)_2$ promotes galena electrochemical dissolution when its concentration is relatively low (<0.10 mol·L^{-1}) and inhibits dissolution at high concentrations (>0.10 mol·L^{-1}) because Pb^{2+} has two different functions during galena electrochemical dissolution: it acts as an oxidant to stimulate cathodic interaction and as an oxidation product that inhibits galena oxidation.

(3) Higher temperatures reduce polarization resistance and decrease charge transform resistance and passive resistance, therefore accelerating galena electrochemical dissolution. The galena corrosion current density increased from 0.143 to 0.226 µA·cm^{-2} when the temperature increased from 25 to 55 °C. This behavior is caused by the increasing temperature, which causes a conversion of the internal energy into electrochemical energy.

References

1. Ralston J (1994) The chemistry of galena flotation-principles-and-practice. Mine Eng 7(5–6):715–735

2. Lar UA, Ngozi-Chika CS, Ashano EC (2013) Human exposure to lead and other potentially harmful elements associated with galena mining at New Zurak, central Nigeria. J Afr Earth Sci 84:13–19

3. Neuberger JS, Mulhall M, Pomatto MC, Sheverbush J, Hassanein RS (1990) Health problems in Galena, Kansas: a heavy metal mining superfund site. Sci Total Environ 94(3):261–272

4. Fang T, Liu GJ, Zhou CC, Sun RY, Chen J, Wu D (2014) Lead in Chinese coals: distribution, modes of occurrence, and environmental effects. Environ Geochem Health 36(3):563–581

5. Benvenuti M, Mascaro I, Corsini F, Lattanzi P, Parrini P, Tanelli G (1997) Mine waste dumps and heavy metal pollution in abandoned mining district of Boccheggiano (Southern Tuscany, Italy). Environ Geol 30(3–4):238–243

6. Luo LQ, Chu BB, Liu Y, Wang XF, Xu T, Bo Y (2014) Distribution, origin, and transformation of metal and metalloid pollution in vegetable fields, irrigation water, and aerosols near a Pb-Zn mine. Environ Sci Pollut Res 21(13):8242–8260

7. Chakroun HK, Souissi F, Souissi R, Bouchardon JL, Moutte J, Abdeljaoued S (2013) Heavy metals distribution and mobility in flotation tailings and agricultural soils near the abandoned Pb-Zn district of Jebel Hallouf-Sidi Bouaouane (NW Tunisia). Carpath J Earth Env 8(3):249–263

8. Boughriet A, Recourt P, Proix N, Billon G, Leermakers M, Fischer JC, Ouddane B (2007) Fractionation of anthropogenic lead and zinc in Deule River sediments. Environ Chem 4(2):114–122

9. Kristensen LJ, Taylor MP, Morrison AL (2015) Lead and zinc dust depositions from ore trains characterised using lead isotopic compositions. Environ Sci Proc Impact 17(3):631–637

10. Lara RH, Briones R, Monroy MG, Mullet M, Humbert B, Dossot M, Naja GM, Cruz R (2011) Galena weathering under simulated calcareous soil conditions. Sci Total Environ 409(19):3971–3979

11. Salamy SG, Nixon JG (1953) The application of electrochemical methods to flotation research. In: Recent developments in mineral dressing. Institution of Mining and Metallurgy, London, 503

12. Mikhlin Y, Kuklinskiy A, Mikhlina E, Kargin V, Asanov I (2004) Electrochemical behaviour of galena (PbS) in aqueous nitric acid and perchloric acid solutions. J Appl Electrochem 34(1):37–46

13. Fornasiero D, Li FS, Ralston J (1994) Oxidation of galena. 2. Electrokinetic study. J Colloid Interface Sci 164(2):345–354

14. Brodie JB (1969) The electrochemical dissolution of Galena. M.Sc. Thesis, University of British Columbia

15. Paul RL, Nicol MJ, Diggle JW, Saunders AP (1978) Electrochemical behavior of galena (lead sulfide). 1. Anodic-dissolution. Electrochim Acta 23(7):625–633

16. Nicol MJ, Paul RL, Diggle JW (1978) Electrochemical behavior of galena (lead sulfide). 2. Cathodic reduction. Electrochim Acta 23(7):635–639

17. Nava JL, Oropeza MT, Gonzalez I (2002) Electrochemical characterisation of sulfur species formed during anodic dissolution of galena concentrate in perchlorate medium at pH 0. Electrochim Acta 47(10):1513–1525

18. Cisneros-Gonzalez I, Oropeza-Guzman MT, Gonzalez I (1999) Cyclic voltammetry applied to the characterisation of galena. Hydrometallurgy 53(2):133–144

19. Cisneros-Gonzalez I, Oropeza-Guzman MT, Gonzalez I (2000) An electrochemical study of galena concentrate in perchlorate medium at pH 2.0: the influence of chloride ions. Electrochim Acta 45(17):2729–2741

20. Gardner JR, Woods R (1979) Study of the surface oxidation of galena using cyclic voltammetry. J Electroanal Chem 100(1–2):447–459

21. Pauporte T, Schuhmann D (1996) A study by impedance spectroscopy of the reactivity of freshly polished galena electrodes: oxidation and interaction with ethylxanthate. J Electroanal Chem 404(1): 123–135

22. Shapter JG, Brooker MH, Skinner WM (2000) Observation of the oxidation of galena using Raman spectroscopy. Int J Miner Process 60(3–4):199–211

23. Higgins SR, Hamers RJ (1995) Spatially-resolved electrochemistry of the lead sulfide (galena) (001) surface by electrochemical scanning-tunneling-microscopy. Surf Sci 324(2–3):263–281

24. Buckley AN, Woods R (1990) X-ray photoelectron spectroscopic and electrochemical studies of the interaction of xanthate with galena in relation to the mechanism proposed by Page and Hazell. Int J Miner Process 28(3–4):301–311

25. Chernyshova IV (2003) An in situ FTIR study of galena and pyrite oxidation in aqueous solution. J Electroanal Chem 558:83–98

26. Kartio I, Laajalehto K, Kaurila T, Suoninen E (1996) A study of galena (PbS) surfaces under controlled potential in pH 4.6 solution by synchrotron radiation excited photoelectron spectroscopy. Appl Surf Sci 93(2):167–177

27. Othmani MA, Souissi F, Benzaazoua M, Bouzahzah H, Bussiere B, Mansouri A (2013) The geochemical behaviour of mine tailings from the Touiref Pb-Zn District in Tunisia in weathering cells leaching tests. Mine Water Environ 32(1):28–41

28. Clevenger TE, Rao D (1996) Mobility of lead in mine tailings due to landfill leachate. Water Air Soil Pollut 91(3–4):197–207

29. Lu JM, Alakangas L, Wanhainen C (2014) Metal mobilization under alkaline conditions in ash-covered tailings. J Environ Manage 139:38–49

30. Bard AJ, Faulkner LR (2001) Electrochemical methods: fundamentals and applications, 2nd edn. Wiley, Hoboken

31. Stern M, Geary AL (1957) Electrochemical polarization. 1. A theoretical analysis of the shape of polarization curves. J Electrochem Soc 104(1):56–63

32. Solmaz R, Kardas G, Yazici B, Erbil M (2008) Adsorption and corrosion inhibitive properties of 2-amino-5-mercapto-1, 3, 4-thiadiazole on mild steel in hydrochloric acid media. Colloid Surf A Physicochem Eng Asp 312(1):7–17

33. Wang XM, Yang HY, Wang FH (2011) An investigation of benzimidazole derivative as corrosion inhibitor for mild steel in different concentration HCl solutions. Corros Sci 53(1):113–121

34. Orazem ME, Tribollet B (2008) An integrated approach to electrochemical impedance spectroscopy. Electrochim Acta 53(25):7360–7366

35. Constantin CA, Chirita P (2013) Oxidative dissolution of pyrite in acidic media. J Appl Electrochem 43(7):659–666

36. Ouyang YT, Liu Y, Zhu RL, Ge F, Xu TY, Luo Z, Liang LB (2015) Pyrite oxidation inhibition by organosilane coatings for acid mine drainage control. Mine Eng 72:57–64

37. Pang J, Briceno A, Chander S (1990) A study of pyrite solution interface by impedance spectroscopy. J Electrochem Soc 137(11): 3447–3455

38. Macdonald JR (1985) Generalizations of "universal dielectric response" and a general distribution-of- activation-energies model for dielectric and conducting systems. J Appl Phys 58:1971–1978

39. Moslemi H, Shamsi P, Habashi F (2011) Pyrite and pyrrhotite open circuit potentials study: effects on flotation. Mine Eng 24(10): 1038–1045

40. Geng M, Duan ZH (2010) Prediction of oxygen solubility in pure water and brines up to high temperatures and pressures. Geochim Cosmochim Acta 74(19):5631–5640

41. Chirita P, Popa I, Duinea MI, Schlegel ML (2014) Electrochemical investigation of the mechanism of aqueous oxidation of pyrite by oxygen. Geochem Earth Surf 10:154–158 **(Ges-10)**